A Membrane Protein, EzrA, Regulates Assembly Dynamics of FtsZ by Interacting with the C-Terminal Tail of FtsZ†

Jay Kumar Singh,‡ Ravindra D. Makde,§ Vinay Kumar,§ and Dulal Panda*,‡

School of Biosciences and Bioengineering, IIT Bombay, Powai, Mumbai 400076, India, and High Pressure Physics Division, Bhabha Atomic Research Centre, Mumbai 400085, India

Received April 16, 2007; Revised Manuscript Received July 20, 2007

ABSTRACT: FtsZ polymerizes to form a dynamic ring structure called the Z-ring at the midcell of bacteria. EzrA, a membrane protein, has been shown to prevent the formation of aberrant Z-rings in the low GC Gram-positive bacteria by inhibiting FtsZ assembly. In this study, we show that *Bacillus subtilis* (*B. subtilis*) EzrA inhibited the assembly and bundling of *B. subtilis* FtsZ. It increased the critical concentration of FtsZ assembly and depolymerized the preformed FtsZ polymers in vitro. We obtained evidence suggesting that *B. subtilis* EzrA forms complex with *B. subtilis* FtsZ in vitro. EzrA was found to bind to FtsZ at a single site with a dissociation constant of $4.3 \pm 0.6\ \mu$M. EzrA−FtsZ interaction has a significant electrostatic contribution as apparent from the effect of salt on their binding interactions. To elucidate the site of interaction between EzrA and FtsZ, we deleted 16 amino acid residues from the extreme C-terminal tail of *B. subtilis* FtsZ, which are conserved in FtsZ orthologues. EzrA did not inhibit the assembly of C-terminal truncated *B. subtilis* FtsZ. It also did not bind to the C-terminal truncated FtsZ detectably, suggesting that EzrA interacts with FtsZ through its conserved C-terminal tail residues. Further, a 17-residue synthetic peptide (365−382) of the C-terminal tail of FtsZ (CTP17) was used to probe the interaction of EzrA with the C-terminal tail of FtsZ. CTP17 bound to EzrA, inhibited the binding of EzrA to FtsZ, and surmounted the inhibitory effects of EzrA on the assembly of FtsZ in vitro. The data together showed that EzrA binds to the C-terminal tail of FtsZ. FtsA, a positive regulator of FtsZ assembly, is also known to interact with the C-terminal tail of FtsZ. The results indicated an interesting possibility that the assembly dynamics of FtsZ in the Z-ring is regulated by the competition between positive and negative regulators sharing the same binding site on FtsZ.

FtsZ, a major cytoskeleton protein present in bacteria, is highly conserved throughout the prokaryotes, and its homologue has also been found in a number of eukaryotic organelles (*1*, *2*). Self-assembled FtsZ forms a highly dynamic ring structure termed the "Z-ring" at the midpoint of bacterial cell (*2*, *3*). Other essential cell division proteins assemble in a hierarchical manner on the Z-ring and form the septum, which empowers the bacterial cytokinesis (*3*, *4*). FtsZ polymerizes reversibly in a GTP-dependent manner in vitro, and the dynamics of FtsZ assembly is thought to be partly regulated by the GTP hydrolysis (*5*−*10*). The assembly dynamics of FtsZ is shown to be influenced by proteins, metal ions, osmolytes, and macromolecular crowding agents (*8*, *11*−*15*).

It is estimated that nearly 30% of the cellular FtsZ is in the Z-ring at a given time (*16*). Increasing the intracellular concentration of FtsZ by 2−5-fold leads to the formation of rings at the cell poles and nonproductive polar septation, and the overexpression of FtsZ has been shown to disrupt the Z-ring formation leading to the cell filamentation (*17*). Thus, the stability of the FtsZ protofilaments is thought to be important for the assembly and localization of FtsZ during the bacterial cell division (*18*). Positive regulators such as FtsA, ZapA, and ZipA (found only in γ-proteobacteria) and negative regulators like SulA, MinCD, and EzrA (found only in low GC Gram-positive bacteria) are shown to influence the assembly dynamics of FtsZ polymers in vivo (*17*−*23*). These regulatory proteins are thought to be critical for the stability and correct positioning of the Z-ring. Several of the positive and negative acting factors are thought to interact with FtsZ directly, but little is known about the sites that are involved in the interactions for the majority of these proteins.

The positive regulators enhance FtsZ polymerization and stabilize the protofilaments. For example, ZapA promotes FtsZ polymerization, filament formation, and stabilization and engages FtsZ molecules with an approximate 1:1 stoichiometry (*24*). It is incorporated into the cytokinetic ring at an early stage of its assembly, possibly interacting with FtsZ directly (*19*). FtsA, another positive regulator of the FtsZ assembly, interacts with the C-terminus tail of FtsZ, and it is the first protein to be recruited at the Z-ring (*24*, *25*).

The negative-acting factors are also critical for maintaining the pool of unassembled FtsZ and for the localization of the

†This work is supported by a grant from the Department of Science and Technology, Government of India, to D.P. and a CSIR doctoral fellowship to J.K.S.

* Corresponding author. Tel: +91-22-2576-7838. Fax: +91-22-2572-3480. E-mail: panda@iitb.ac.in.

‡ School of Biosciences and Bioengineering, IIT Bombay.

§ High Pressure Physics Division, Bhabha Atomic Research Centre.

10.1021/bi700710j CCC: $37.00
Published on Web 08/24/2007

Z-ring. Polar FtsZ assembly in *B. subtilis* is inhibited by the Min system (Min CD and DivIVA that is a functional homologue of *Escherichia coli* MinE) (*16*). The Min system is needed to prevent polar division, but it is not required for the accurate placement of the division site at the midcell in *Bacillus subtilis* during sporulation (*26*). The inhibition of cell division caused by overexpression of MinCD is suppressed by *ezrA* null mutation (*27*). The EzrA protein is a membrane-anchoring protein and is also known to be involved in the spatial regulation of the Z-ring formation in *B. subtilis* (*18*). It has been shown that the null mutation in *ezrA* results in the formation of extra Z-rings by lowering the critical concentration of FtsZ assembly (*18*).

EzrA is conserved throughout the low GC Gram-positive bacteria and is uniformly distributed throughout the plasma membrane, while Min proteins are localized site-specifically (*17*, *27*). The EzrA protein concentrates at the cytokinetic ring in an FtsZ-dependent manner during the cell division, which provides the evidence for direct interaction between EzrA and FtsZ (*18*). It has been reported that purified EzrA inhibited the FtsZ polymerization in vitro (*17*, *28*). The mechanism of EzrA induced inhibition of FtsZ polymerization and the site of interaction, however, have not been elucidated.

In this study, we used native *B. subtilis* FtsZ, 16 C-terminal residue truncated *B. subtilis* FtsZ, and a 17-residue synthetic peptide (365−382) of the C-terminal tail of FtsZ to elucidate the mechanism of inhibition of FtsZ polymerization by EzrA. EzrA reduced the assembly and bundling of native FtsZ and depolymerized the preformed protofilaments in vitro. We present evidence suggesting that EzrA binds to FtsZ and that EzrA inhibits the assembly of FtsZ by sequestration of soluble FtsZ monomers. EzrA had minimal effects on the assembly of truncated FtsZ that lacked the 16 C-terminal tail residues. A 17-mer FtsZ synthetic peptide (365−382) countered the inhibitory effects of EzrA on the assembly of FtsZ, suggesting that EzrA-induced inhibition of FtsZ polymerization occurred through its binding at the conserved C-terminal tail of FtsZ. It is known that several positive regulators like FtsA also bind to the C-terminal tail of FtsZ. Therefore, it is logical to consider that the positive regulators may overcome the negative effect of EzrA on the FtsZ assembly at the midcell, permitting the formation of a medial Z-ring.

EXPERIMENTAL PROCEDURES

Materials. Piperazine-*N*,*N*′-bis(2-ethanesulfonic acid) (Pipes),[1] *N*-(2-hydroxyethyl)piperazine-*N*′-2-ethanesulfonic acid (Hepes), phenylmethanesulfonyl fluoride (PMSF), bovine serum albumin (BSA), β-mercaptoethanol (β-ME), DEAE-dextran, and GTP were purchased from Sigma. Sephadex G-150 and CNBr-activated Sepharose 4B were purchased from Pharmacia Fine Chemicals and Pharmacia LKB Biotechnology, respectively. Bio-Gel P-6 resin was purchased from Bio-Rad Laboratories, and Ni-NTA coupled to Sepharose CL-6B was from QIAGEN. Acrylodan was purchased from Molecular Probes. All other chemicals used were of analytical grade. *B. subtilis* ATCC6633 was obtained from the Institute of Microbial Technology, Chandigarh, India.

Cloning and Overexpression of ftsZ and ezrA Genes. E. coli XL1 Blue was used as the cloning host. The genomic DNA of *B. subtilis* ATCC6633 was used for the PCR amplifications of the desired *orf*s using *Pfu* turbo DNA polymerase. The fzbs1 (AGGAGGATTTCATATGTTGGAGTTCG) and fzbs2 (TTGTCCGGATCCTTAGCCGCGTTTATTAC) and fzbs1 and fzbs3 (ATGTCGGATCCTTAATCAGCCGGCTGTGAAG) primer pairs were used to amplify the full-length and 3′ truncated *orf*s of *ftsZ*. These were cloned into the *Nde*I and *Bam*HI site of the pET16b plasmid. The 3′ truncation in the *ftsZ* gene was engineered for the expression of the truncated FtsZ (FtsZΔC16) protein that lacks the 16-residue C-terminal tail. The recombinant plasmids were subsequently transformed into BL21(DE3) pLysS for the overexpression of native FtsZ and FtsZΔC16 proteins. The ezbs1 (ACAAGCTCCATATGATCTACGCCGAAATCGACCGG) and ezbs2 (GCATGGATCCTTAAGCGGATATGTCAGCTTTGA) primer pair was used to amplify the 5′ truncated *orf* of *ezrA* from the pRS3 plasmid (*17*) for expressing truncated EzrA lacking the 24 residue long membrane anchoring N-terminal region of the wild-type EzrA. Since the N-terminal truncated EzrA is functionally active and inhibits FtsZ polymerization, we have referred it as EzrA throughout the text. This *orf* was subsequently cloned into the *Nde*I and *Bam*HI site of pET28a(+). The recombinant plasmid was later transformed into the BL21(DE3) host for the overexpression of EzrA. The expressed FtsZ, FtsZΔC16, and EzrA proteins carry polyhistidine tags fused at their N-termini. The constructs were sequenced using an automated DNA sequencer (ABI-PRISM 377). The sequence of the genomic *ftsZ* of the *B. subtilis* ATCC6633 strain, which matches exactly with our construct, has been deposited in GenBank with the accession number EF612436. The deduced amino acid sequence of expressed FtsZ matches with *B. subtilis* strain 168 (ATCC23857) except for three changes (P325S, D345E, and A346P), which are localized in the variable domain of the FtsZ protein.

Purification of B. subtilis FtsZ (Native as well as C-Terminal Truncated) and EzrA Proteins. Recombinant native FtsZ and C-terminal truncated FtsZ (FtsZΔC16) proteins of *B. subtilis* were overexpressed and purified from *E. coli* BL21(DE3)pLysS clones individually. The cells containing the desired constructs were grown at 37 °C in LB media containing 12.5 μg/mL chloramphenicol and 100 μg/mL ampicillin. The cells were induced at the late log phase (OD_{600} ~0.8) by the addition of 0.5 mM IPTG and incubated for an additional 4 h. Subsequently, the cells were harvested by centrifugation at 10000*g* at 4 °C for 15 min. The cell pellet was washed with lysis buffer (50 mM NaH_2PO_4, pH 8.0, and 300 mM NaCl), resuspended in ice-cold lysis buffer containing 0.1% β-ME and 2 mM PMSF, and homogenized for 5 min on ice. The cell suspension was incubated with 1 mg/mL lysozyme for 1 h on ice. Cells were disrupted by ultrasonication with ten pulses of 30 s each at 30 s intervals. The lysate was cleared by centrifugation at 120000*g* for 30 min at 4 °C. Imidazole (5 mM) was added to the cleared

[1] Abbreviations: FtsZΔC16, C-terminal 16-residue truncated FtsZ; CTP17, C-terminal tail peptide (DDTLDIPTFLRNRNKRG) of FtsZ; Pipes, piperazine-*N*,*N*′-bis(2-ethanesulfonic acid); Hepes, *N*-(2-hydroxyethyl)piperazine-*N*′-2-ethanesulfonic acid; IPTG, isopropyl β-D-thiogalactopyranoside; β-ME, β-mercaptoethanol; BSA, bovine serum albumin; GTP, guanosine 5′-triphosphate; Ni-NTA, nickel(II) nitrilotriacetic acid; DEAE-dextran, diethylaminoethyl-dextran.

supernatant. The supernatant was loaded onto a Ni-NTA agarose column. The column was washed extensively with a buffer containing 25 mM Pipes, pH 6.8, 300 mM NaCl, and 10 and 25 mM imidazole. Protein was eluted with a discontinuous gradient of imidazole (50, 100, 250, and 500 mM). Native FtsZ and FtsZΔC16 proteins were eluted with 100 mM imidazole. The fractions containing the desired proteins were pooled, and salts were removed by gel filtration column chromatography using Bio-Gel P-6 resin. The protein was concentrated using Amicon Ultra PL-10 (Millipore) at 4 °C. Both native FtsZ and FtsZΔC16 proteins were estimated to be ≥97% pure by SDS−PAGE. The purified FtsZ and FtsZΔC16 concentrations were determined through the Bradford method using BSA as a standard (*29*), and the final concentrations of FtsZ and FtsZΔC16 were calculated using a correction factor of 1.2 for the BSA/FtsZ ratio (*30*). Finally, the purified proteins were aliquoted and stored at −80 °C.

The recombinant *B. subtilis* EzrA protein was overexpressed and purified from the *E. coli* BL21(DE3) strain (*17*). Briefly, the cells grown at 37 °C in LB media were induced with 0.5 mM IPTG. The Cells were lysed by ultrasonication with 30 pulses at 30 s intervals. The clear supernatant of lysed cells containing 5 mM imidazole was loaded onto a Ni-NTA agarose column. The EzrA protein was eluted after extensive washing of the column in a discontinuous gradient of imidazole of 25, 75, 150, and 250 mM. The EzrA protein was found to be eluted with 75 and 150 mM imidazole. Salts from the pooled EzrA fractions were removed by using the Bio-Gel P-6 resin. The protein was concentrated using Amicon Ultra PL-10 (Millipore) at 4 °C. The purity of EzrA was estimated to be ≥98% by SDS−PAGE. The concentration of EzrA was determined by measuring the absorbance at 278 nm using 45920 M^{-1} cm^{-1} as the molar extinction coefficient, which was determined considering the number of tyrosine, tryptophan, and cysteine residues present. We estimated the EzrA concentration by the Bradford method using BSA as a standard (*29*), and this concentration of EzrA was finally adjusted using a correction factor of 1.2 for the BSA/EzrA ratio. Purified EzrA was stored at −80 °C.

The integrity of the purified FtsZ, FtsZΔC16, and EzrA proteins was confirmed by Axima-CFR MALDI-TOF-MS (Kratos Analytical, Manchester, U.K.). The molecular masses of the FtsZ, FtsZΔC16, and EzrA proteins were determined to be 42.7, 40.7, and 64.1 kDa, respectively. The measured molecular masses matched well with the calculated molecular weights of the protein sequences deduced from the DNA sequences.

Light Scattering Signal. The effects of EzrA on the assembly of native FtsZ and FtsZΔC16 were monitored by 90° light scattering signals using a JASCO 6500 spectrofluorometer. FtsZ (14.4 μM) or FtsZΔC16 (14.4 μM) was incubated without or with different concentrations (0.6, 1.2, 3.6, and 7.2 μM) of EzrA in 25 mM Pipes buffer, pH 6.8, for 30 min on ice. After 30 min of incubation, 10 mM $MgCl_2$ and 1 mM GTP were added to the reaction mixture, and the reaction mixture was immediately transferred into a quartz cuvette (Sterna Cells) for monitoring the light scattering signal at 37 °C for 10 min at 500 nm.

Sedimentation Assay. B. subtilis FtsZ, FtsZΔC16, and EzrA were precleared by spinning at 280000*g* for 10 min at 4 °C. The prepared reaction milieu of native FtsZ or FtsZΔC16 (7.2 μM) proteins in 25 mM Pipes buffer, pH 6.8, was incubated in the presence of different concentrations (0, 1.2, 3.6, 7.2 μM) of EzrA for 30 min on ice. After 30 min of incubation, 10 mM $MgCl_2$ and 1 mM GTP were added to the reaction mixtures and incubated for an additional 15 min at 37 °C. FtsZ polymers were sedimented at 280000*g* for 30 min at 30 °C. The supernatant was decanted carefully without disturbing the pellet. The pellet was washed once with 25 mM Pipes buffer, pH 6.8, at 37 °C carefully, and it was dissolved in 25 μL of ice-cold 25 mM Pipes buffer, pH 6.8. The protein concentrations of the pellet and supernatant were estimated from the Coomassie blue staining of the SDS−PAGE using a gel documentation system from Kodak Digital Science.

Visualization of FtsZ Polymers by Transmission Electron Microscopy. Native FtsZ (14.4 μM) or FtsZΔC16 (14.4 μM) was incubated in 25 mM Pipes buffer, pH 6.8, in the absence and presence of different concentrations (1.2, 3.6, and 7.2 μM) of EzrA for 15 min on ice. Then, 10 mM $MgCl_2$ and 1 mM GTP were added to the reaction mixtures and immediately placed at 37 °C for 10 min. The sample for electron microscopy was prepared as described previously (*31*). The samples were analyzed using 120v TECNAI G^2 12 FEI TEM.

Effects of EzrA on the Critical Concentration of FtsZ Polymerization. The reaction milieus of different concentrations (2.4, 4.8, 7.2, 9.6, 12, and 14.4 μM) of FtsZ were incubated without or with 3.6 μM EzrA in 25 mM Pipes buffer at pH 6.8 for 30 min on ice. After 30 min of incubation, 10 mM $MgCl_2$ and 1 mM GTP were added to the reaction mixtures and were immediately transferred to 37 °C. After 10 min of assembly, FtsZ polymers were sedimented for 20 min at 280000*g*. The amount of FtsZ pelleted was quantified by Coomassie blue staining of 10% SDS−polyacrylamide gel electrophoresis using Image J 1.32j software. The intensity of Coomassie blue staining of FtsZ was expressed as the FtsZ concentration unit using a known FtsZ standard.

Effect of EzrA on Preformed Polymers of FtsZ. FtsZ (14.4 μM) was polymerized in 25 mM Pipes buffer, pH 6.8, containing 10 mM $MgCl_2$ and 1 mM GTP at 37 °C. The assembly kinetics of FtsZ was followed by monitoring light scattering at 500 nm. At the steady state, 1.2 μM EzrA was added to the reaction milieu, and the light scattering intensity was monitored for an additional 400 s. Finally, 6 μM EzrA was added to the same reaction milieu, and the light scattering signal was monitored for an additional 400 s.

Monitoring FtsZ−EzrA Interactions by Size-Exclusion Chromatography. FtsZ (7.2 μM) was incubated with EzrA (14.4 μM) in buffer A (25 mM Pipes buffer, pH 6.8, containing 50 mM NaCl) for 30 min on ice. The protein mixture was loaded onto a Sephadex G-150 column (1 × 43 cm) preequilibrated with buffer A. The proteins were eluted at the flow rate of 0.8 mL min^{-1} in 0.8 mL fractions each. The protein concentration of each fraction was measured using the Bradford method (*29*). The elution profiles of FtsZ and EzrA were also individually monitored using the same column. The elution profiles of the FtsZ−EzrA complex, EzrA, and FtsZ were distinctly different. The eluted proteins were judged on 10% SDS−PAGE.

Chemical Modification of the Cysteine Residue of EzrA by Acrylodan. The single cysteine residue (at position 276)

of EzrA was labeled by incubating EzrA with a 10-fold molar excess of acrylodan at 25 °C for 3 h in 50 mM Hepes buffer, pH 8.0. The labeling reaction was stopped by adding 1 mM β-ME. The reaction mixture was spun at 50000*g* for 20 min at 4 °C to remove any aggregate formed during the chemical modification. The unbound acrylodan molecules were removed by passing through a gel filtration (Bio-Gel P-6 resin) column followed by dialysis against 50 mM Hepes buffer, pH 7.5, for 8 h at 4 °C. The concentration of EzrA was measured by the Bradford assay (*29*), and the concentration of EzrA-bound acrylodan was determined by using an extinction coefficient of 20000 M^{-1} cm^{-1} at 392 nm. Incorporation stoichiometry was calculated by dividing EzrA bound acrylodan concentration by the protein concentration. The labeling efficiency of EzrA by acrylodan was found to be 0.55 ± 0.12.

Determination of the Dissociation Constant of the EzrA and FtsZ Interaction. Acrylodan−EzrA (1.2 μM) was incubated in 25 mM Pipes buffer, pH 6.8, in the absence and presence of different concentrations (1.2−19.2 μM) of either FtsZ or FtsZΔC16 for 30 min on ice. After 30 min of incubation, the fluorescence spectra were recorded in the range of 450−550 nm using 390 nm as an excitation wavelength. We used 5 and 10 nm for excitation and emission band widths, respectively. The increased acrylodan−EzrA fluorescence at 490 nm upon binding to FtsZ was used to determine the dissociation constant (K_d) of the EzrA and FtsZ interaction using the equation:

$$\Delta F = \Delta F_{max} L/(K_d + L)$$

where ΔF is change in the fluorescence intensity of the acrylodan−EzrA upon binding to FtsZ, ΔF_{max} is the maximum change in the fluorescence intensity of acrylodan−EzrA when it is fully liganded with FtsZ, and L is the concentration of FtsZ. The ΔF_{max} value (21.3 ± 1) was calculated by the GraphPad Prism 5 software. ΔF was calculated by subtracting the fluorescence intensity of acrylodan−EzrA in the absence of FtsZ from the fluorescence intensity of acrylodan−EzrA in the presence of different concentrations of FtsZ. The data were statistically analyzed and curve fitted using GraphPad Prism 5 software.

Job's Plot. The stoichiometry of EzrA binding to FtsZ was determined using the method of continuous variation (*32*, *33*). Mixtures of different molar ratios of the FtsZ and EzrA proteins were prepared such that the total concentration of these proteins was constant at 6 μM. The reaction solutions were incubated for 30 min at 25 °C. Then, the fluorescence intensity was measured at 490 nm using 390 nm as an excitation wavelength.

Competition-Based Peptide Binding Assay. Using Fmoc chemistry, CTP17 peptide (corresponding to amino acids 365−382 of *B. subtilis* FtsZ) was synthesized by solid-phase peptide synthesis procedures (USV-Custom, Mumbai, India). The synthetic peptide was purified by RP-HPLC using a pore (100 Å) and C18 column. The theoretical and measured (MALDI-TOF-MS) molecular masses of CTP17 were 2031 and 2038 Das, respectively. The peptide was dissolved in 25 mM Pipes buffer, pH 6.8. The purity level of the peptide was found to be ≥95%.

EzrA (7.2 μM) was incubated without or with different concentrations (10−100 μM) of CTP17 in 25 mM Pipes buffer, pH 6.8, for 30 min on ice. FtsZ (14.4 μM) was added to each of the reaction mixtures and incubated for an additional 30 min on ice. Then, 10 mM $MgCl_2$ and 1 mM GTP were added to each of the reaction mixtures, and the assembly kinetics of FtsZ was monitored by light scattering at 37 °C. To examine the effect of CTP17 on FtsZ polymerization, FtsZ (14.4 μM) was incubated with CTP17 (100 μM) in 25 mM Pipes buffer, pH 6.8, for 30 min on ice. Then, 10 mM $MgCl_2$ and 1 mM GTP were added to the reaction milieu. The kinetics of FtsZ assembly was monitored at 37 °C.

Acrylodan−EzrA (1.2 μM) was incubated without or with different concentrations (5, 10, 15, 25, 50, 75, 100, and 200 μM) of CTP17 for 30 min in 25 mM Pipes buffer, pH 6.8. The emission spectra (450−550 nm) were recorded using 390 nm as an excitation wavelength. Like native FtsZ, CTP17 also increased the fluorescence intensity of acrylodan−EzrA in a concentration-dependent fashion. The change in the fluorescence intensity of acrylodan−EzrA upon binding to CTP17 was used to determine the dissociation constant of their binding interaction as described previously. The binding data were statistically analyzed and curve fitted using GraphPad Prism 5 software.

Monitoring the Interaction between EzrA and CTP17 Using EzrA Coupled with CNBr-Activated Sepharose 4B. The coupling of EzrA with CNBr-activated Sepharose 4B was done using the manufacturer protocol (Pharmacia LKB Biotechnology). Briefly, CNBr-activated Sepharose 4B beads were swelled and washed with 1 mM HCl and then equilibrated with coupling buffer (0.1 M $NaHCO_3$, pH 8.5, containing 0.5 M NaCl). EzrA (3.6 μM) was incubated with CNBr-activated Sepharose 4B at 4 °C overnight in coupling buffer. These beads were washed with coupling buffer and were incubated for 4 h with blocking agent (0.2 M glycine, pH 8.0) at 4 °C. Subsequently, the beads were washed with 0.1 M acetate buffer, pH 4.0, containing 0.5 M NaCl and were again washed three times with the coupling buffer.

EzrA coupled with Sepharose 4B beads was used to elucidate interactions between EzrA and FtsZ or CTP17. EzrA coupled with Sepharose 4B beads was divided into three fractions. FtsZ (7.2 μM) was incubated with one of these fractions for 2 h on ice. The other two fractions were incubated with 100 and 300 μM CTP17 for 2 h and subsequently incubated with FtsZ (7.2 μM) for an additional 2 h on ice. The protein-bound beads were thoroughly washed with coupling buffer and were suspended in SDS sample loading buffer. The samples were analyzed by Coomassie blue staining on 10% SDS−PAGE.

Effects of Sodium Chloride on the Binding of FtsZ and EzrA. Acrylodan−EzrA (1.2 μM) was incubated in the absence and presence of FtsZ (2.4 μM) for 30 min on ice in 25 mM Pipes buffer, pH 6.8. The solutions were then incubated without or with different concentrations (0.1−1 M) of sodium chloride for an additional 30 min, and the fluorescence spectra were recorded using 390 nm as an excitation wavelength.

RESULTS

Effect of EzrA on FtsZ Polymerization. The effects of EzrA on the inhibition of FtsZ polymerization were analyzed by 90° light scattering, sedimentation assays, and transmission

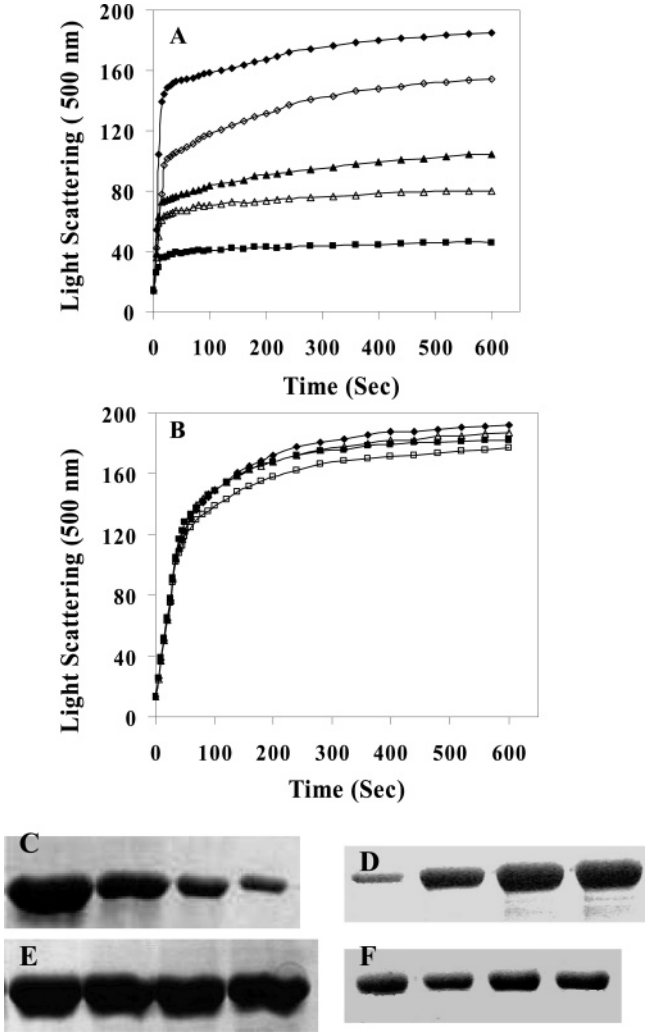

FIGURE 1: EzrA inhibited the assembly of FtsZ. Effects of EzrA on the assembly kinetics of the native FtsZ and FtsZΔC16 in 25 mM Pipes buffer, pH 6.8, are shown in panels A and B, respectively. Panel A shows the polymerization of native FtsZ (14.4 μM) in the absence (◆) and presence of 0.6 μM (◇), 1.2 μM (▲), 3.6 μM (△), and 7.2 μM (■) EzrA, respectively. Panel B shows the polymerization of FtsZΔC16 (14.4 μM) in the absence (◆) and presence of 1.2 μM (△), 3.6 μM (■), and 7.2 μM (□) EzrA, respectively. FtsZ or FtsZΔC16 polymers were sedimented, and the amount of polymerized or unpolymerized proteins was quantified by Coomassie blue staining of the 10% SDS−PAGE as described in the Experimental Procedures. Panels C and E show the inhibition of polymeric mass of native FtsZ (7.2 μM) or FtsZΔC16 (7.2 μM) in the absence and presence of 1.2, 3.6, and 7.2 μM EzrA, respectively. The Coomassie blue staining of the soluble FtsZ and FtsZΔC16 in the supernatant fractions is shown in panels D and F, respectively. Seventy-five percent of the total native FtsZ was pelleted in the absence of EzrA.

electron microscopy. Native FtsZ or FtsZΔC16 was mixed with varying concentrations of EzrA, and the assembly of FtsZ was induced by the addition of GTP at 37 °C. EzrA inhibited the rate and extent of the assembly of the native FtsZ in a concentration-dependent fashion as observed by 90° light scattering signals (Figure 1A). The light scattering intensity decreased by 36 ± 5%, 55 ± 2.6%, and 70 ± 6% in the presence of 1.2, 3.6, and 7.2 μM EzrA, respectively, as compared to the control (in the absence of EzrA). To examine whether the decrease in the light scattering intensity is due to the inhibition of the assembly of FtsZ or due to the change in the morphology of FtsZ protofilaments, the

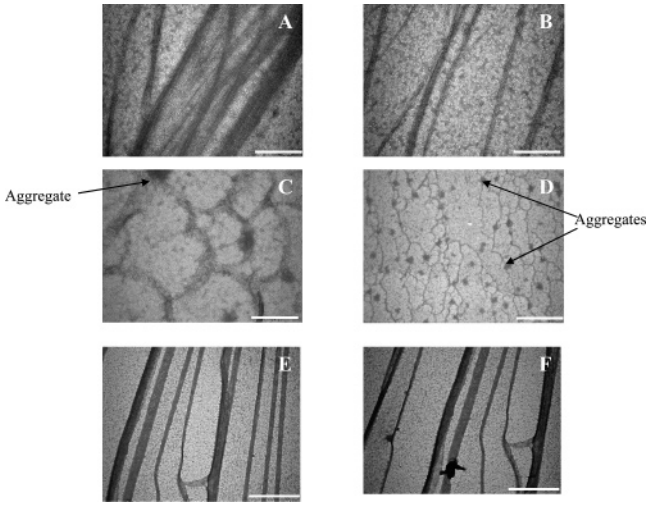

FIGURE 2: Transmission electron micrographs of FtsZ polymers in the absence and presence of EzrA. FtsZ or FtsZΔC16 (14.4 μM) was polymerized in the presence of different concentrations (0, 1.2, 3.6, and 7.2 μM) of EzrA at 37 °C for 10 min in 25 mM Pipes buffer, pH 6.8, containing 1 mM GTP and 10 mM $MgCl_2$. The samples were prepared for electron microscopy as described in the Experimental Procedures. Panels A, B, C, and D represent native FtsZ polymers in the presence of 0, 1.2, 3.6, and 7.2 μM EzrA and panels E and F represent FtsZΔC16 polymers in the presence of 0 and 7.2 μM EzrA, respectively. The scale bar is 2 μm.

polymeric mass of assembled FtsZ polymers was quantified in the absence and presence of different concentrations of EzrA (Figure 1C,D). EzrA reduced the amount of sedimentable polymeric mass of FtsZ in a concentration-dependent fashion. For example, the sedimentable FtsZ polymeric mass reduced by 25 ± 2.5%, 56 ± 4%, and 82 ± 5% in the presence of 1.2, 3.6, and 7.2 μM EzrA, respectively (Figure 1C). Further, EzrA reduced both the length of the FtsZ protofilaments and the extent of the bundling of FtsZ protofilaments (Figure 2A−D). Polymers were barely visible under the microscopic view when the molar ratio of FtsZ and EzrA proteins used was 2:1 (Figure 2D). The results showed that EzrA inhibited both the assembly and bundling of FtsZ protofilaments.

In contrast to the inhibition of the assembly of the native FtsZ, EzrA did not significantly influence the assembly kinetics of FtsZΔC16 that lacked 16 amino acid residues from its C-terminal tail (Figure 1B). For example, the light scattering of FtsZΔC16 polymers decreased by 5.3 ± 1.2% and 7.7 ± 1.3% in the presence of 3.6 and 7.2 μM EzrA, respectively, as compared to the control (Figure 1B). Sedimentation analysis also showed that EzrA did not significantly affect the assembly of FtsZΔC16 (Figure 1E,F). For example, the polymeric mass of FtsZΔC16 was reduced only by 9 ± 3.4% in the presence of 7.2 μM EzrA (Figure 1E). In addition, electron microscopic analysis of the assembly reaction showed no significant change in the size of FtsZΔC16 bundles or in the number of polymers per field view in the absence and presence of 7.2 μM EzrA (Figure 2E,F). The results together demonstrated that EzrA strongly inhibited the polymerization of the native FtsZ but did not inhibit the polymerization of FtsZΔC16 and indicated that FtsZ may interact with EzrA through the C-terminal tail of FtsZ.

EzrA Increased the Critical Concentration of FtsZ Polymerization. The critical concentrations of FtsZ assembly

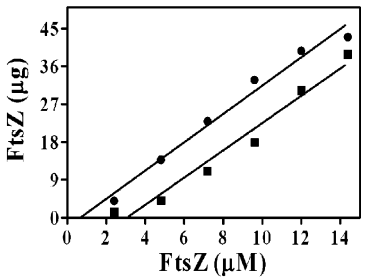

FIGURE 3: Effects of EzrA on the critical concentration of *B. subtilis* FtsZ polymerization. The symbols (●) and (■) represent the sedimentable polymeric mass of FtsZ in the absence and presence of 3.6 μM EzrA, respectively.

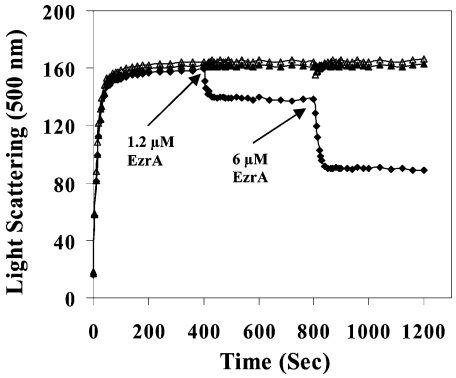

FIGURE 4: EzrA caused the disassembly of the preformed FtsZ protofilaments. FtsZ (14.4 μM) was polymerized in 25 mM Pipes buffer, pH 6.8, containing 1 mM GTP and 10 mM $MgCl_2$ as described in the Experimental Procedures. The arrow indicates the addition of 1.2 and 6 μM EzrA to the preassembled polymers of FtsZ after 400 and 800 s of assembly, respectively (◆). Addition of equal volumes of buffer had no effect on the preformed polymers (△). The trace (▲) represents the assembly kinetics of FtsZ in the absence of EzrA.

in the absence and presence of EzrA were determined using sedimentation assay (Figure 3). Under the experimental conditions used, the critical concentration of FtsZ was determined to be 0.75 ± 0.3 μM. The critical concentration of FtsZ assembly was found to be 3.0 ± 0.6 μM in the presence of 3.6 μM EzrA. Thus, the critical concentration of FtsZ polymerization was found to increase by 4-fold in the presence of 3.6 μM EzrA.

Effect of EzrA on Preformed Polymers of FtsZ. EzrA was added to the preformed FtsZ polymers at different time intervals. EzrA induced the disassembly of the preformed FtsZ polymers in a concentration-dependent fashion (Figure 4). For example, EzrA (7.2 μM) reduced the light scattering signal of the preformed FtsZ polymers by 45% as compared to the control (no EzrA). The reduction in the light scattering is not due to the dilution effects as the addition of an equal amount of buffer did not cause a decrease in the light scattering intensity of the assembled polymers, suggesting that EzrA destabilized the FtsZ polymers and caused the disassembly of the preformed protofilaments.

Characterization of the EzrA and FtsZ Interaction. The interaction of EzrA and FtsZ was examined by size-exclusion chromatography (Figure 5). FtsZ, EzrA, and FtsZ in the presence of EzrA had distinct elution profiles (Figure 5A). For example, FtsZ, EzrA, and the FtsZ−EzrA complex were found to elute at fractions 28, 18, and 11, respectively. The results suggested that EzrA interacts with FtsZ directly.

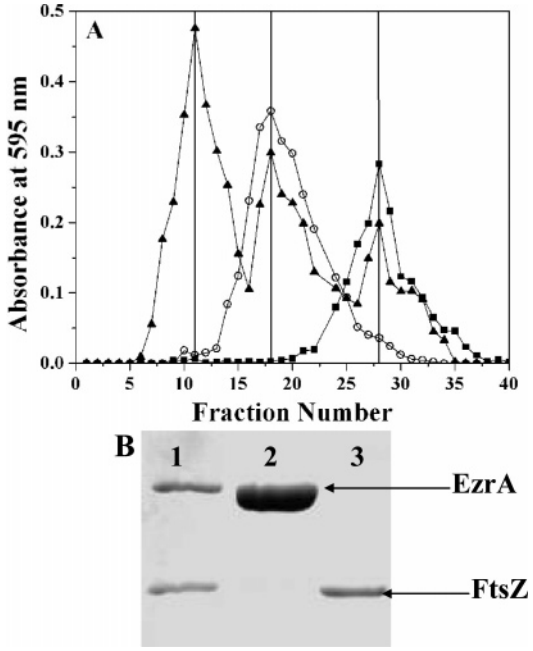

FIGURE 5: Binding of FtsZ to EzrA. Panel A shows the elution profiles of FtsZ (■), EzrA (○), and EzrA-bound FtsZ (▲). FtsZ (7.2 μM) was incubated with EzrA (14.4 μM) for 30 min on ice and passed through a size-exclusion (Sephadex G-150) column (as described in the Experimental Procedures). Panel B shows the Coomassie blue staining of the 10% SDS−PAGE of the FtsZ−EzrA complex (lane 1), EzrA alone (lane 2), and FtsZ alone (lane 3).

Further, the presence of the FtsZ−EzrA complex in the FtsZ/EzrA mixture showed that the protein complex was stable under in vitro conditions (Figure 5B). The elution profiles of the FtsZ and EzrA mixture also showed the presence of uncomplexed FtsZ and EzrA, and their elution peaks matched with the characteristic elution of the individual FtsZ or EzrA.

Acrylodan−EzrA was found to inhibit the assembly kinetics of FtsZ to a similar extent as that of the unlabeled EzrA, suggesting that the covalent modification of EzrA by acrylodan did not affect the functional activity of EzrA (Figure 6A). The fluorescence intensity of the acrylodan−EzrA increased in the presence of FtsZ, indicating that the microenvironment of acrylodan−EzrA changed upon association with FtsZ. Preincubation of EzrA with FtsZ inhibited the increase in the fluorescence intensity of acrylodan−EzrA, suggesting that EzrA and acrylodan−EzrA compete for the same binding site on FtsZ (Figure 6B).

Native FtsZ was found to increase the fluorescence intensity of acrylodan−EzrA in a concentration-dependent manner (Figure 7A). A dissociation constant of the interaction between FtsZ and acrylodan−EzrA was determined to be 4.3 ± 0.6 μM using the fluorescence change (Figure 7B). The stoichiometry of binding was constrained to 1 while fitting the dissociation constant. The stoichiometry of binding was confirmed using the method of continuous variation (*32*). The Job's plot yielded a single binding site for EzrA on FtsZ (Figure 7C). In contrast, FtsZΔC16 did not change the fluorescence intensity of acrylodan−EzrA, suggesting that EzrA did not interact with FtsZΔC16 (Figure 7A). The result suggested that the C-terminal 16 residues are important for the binding of FtsZ to EzrA.

Interaction of EzrA and CTP17. We hypothesized that if the primary binding site of EzrA resides at the C-terminal

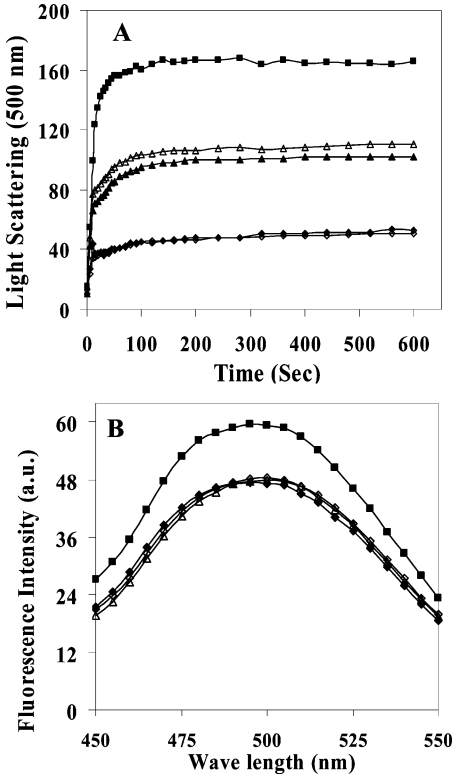

FIGURE 6: Panel A shows the effects of acrylodan−EzrA on the assembly kinetics of native FtsZ. FtsZ (14.4 μM) was polymerized in the absence (■) and in the presence of 1.2 μM (Δ) and 7.2 μM (◆) acrylodan−EzrA or 1.2 μM (▲) and 7.2 μM (◇) EzrA. Panel B shows the competition between acrylodan−EzrA and EzrA for binding to FtsZ monitored by fluorescence spectroscopy. The emission spectra of 1.2 μM acrylodan−EzrA alone (◆), 1.2 μM acrylodan−EzrA plus 3.6 μM FtsZ (■), and 1.2 μM acrylodan−EzrA plus 3.6 μM FtsZ in the presence of 7.2 (△) and 10.8 μM EzrA (◇) are shown.

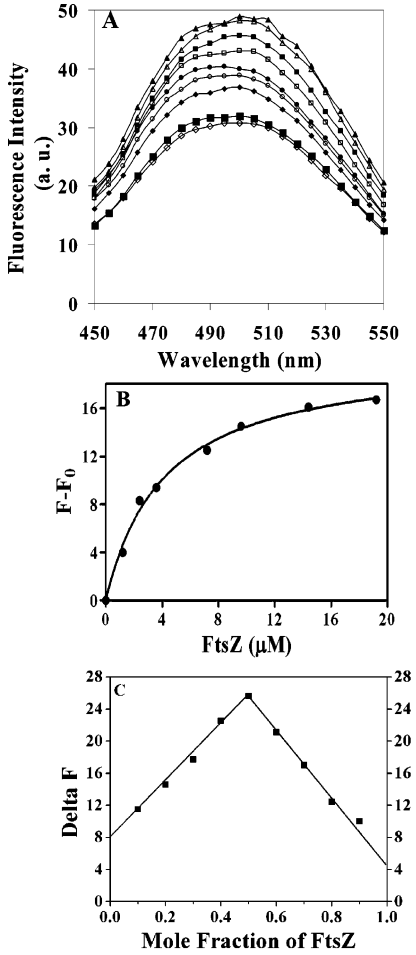

FIGURE 7: Binding of FtsZ to EzrA was monitored by fluorescence spectroscopy. The fluorescence emission spectra of acrylodan−EzrA (1.2 μM) in the absence (◇) and presence of different concentrations of FtsZ, 1.2 μM (◆), 2.4 μM (○), 3.6 μM (●), 7.2 μM (□), 9.6 μM (■), 14.4 μM (△), and 19.2 μM (▲), are shown in panel A. In contrast, FtsZΔC16 (14.4 μM) had no effect on the emission spectra of acrylodan−EzrA (■). Panel B shows the change in the fluorescence intensity of acrylodan−EzrA (1.2 μM) in the presence of different concentrations of FtsZ. The graph was model fitted, and the dissociation constant was determined as described in the Experimental Procedures. The number of binding sites of EzrA per FtsZ was determined by Job's plot (panel C). The concentrations of EzrA and FtsZ were varied continuously, keeping the total concentration of FtsZ plus EzrA constant at 6 μM. The fluorescence intensities were taken at 490 nm and were plotted against the mole fraction of FtsZ. Average values of four individual experiments are shown.

tail of FtsZ, then a synthetic peptide having a sequence similar to that of the C-terminal tail of FtsZ should be able to compete with FtsZ for its binding to EzrA. CTP17, a 17-mer C-terminal (365−382) FtsZ peptide having the amino acid sequence DDTLDIPTFLRNRNKRG, had no detectable effect on the assembly kinetics of native FtsZ in the absence of EzrA (Figure 8A). However, as expected, it prevented the inhibitory effects of EzrA on the assembly of native FtsZ in a concentration-dependent manner. For example, EzrA (7.2 μM) failed to inhibit the assembly of FtsZ in the presence of 100 μM CTP17, suggesting that the peptide blocked the binding of EzrA to FtsZ (Figure 8A). The interaction between CTP17 and EzrA was also examined using fluorescence spectroscopy. CTP17 increased the fluorescence intensity of the acrylodan−EzrA in a concentration-dependent manner (Figure 8B), and a dissociation constant of 102 ± 29 μM was determined for the interaction between CTP17 and acrylodan−EzrA.

Further, the competition between CTP17 and FtsZ for binding to EzrA was investigated by a coprecipitation experiment using EzrA coupled with Sepharose 4B beads (Figure 8C). FtsZ was coprecipitated with EzrA coupled with Sepharose 4B beads, indicating that FtsZ forms a complex with EzrA (lane 1 of Figure 8C). Preincubation of CTP17 with EzrA coupled with Sepharose 4B beads reduced the amount of FtsZ precipitated with EzrA in a concentration-dependent manner, suggesting that CTP17 inhibited the binding of FtsZ to EzrA (lanes 2 and 3 of Figure 8C). These results show that CTP17 inhibits the binding of EzrA to FtsZ and indicate that CTP17 directly interacts with EzrA.

Nature of the Interaction between FtsZ and EzrA. The fluorescence intensity of the acrylodan−EzrA−FtsZ complex decreased with increasing concentration of sodium chloride (Figure 9). However, the fluorescence intensity of acrylodan−EzrA was reduced only minimally in the presence of sodium chloride. Therefore, the decrease in the fluorescence intensity of the acrylodan−EzrA−FtsZ complex in the presence of sodium chloride was not due to the quenching of the fluorescence intensity of acrylodan−EzrA but was due to the inhibition of the FtsZ−EzrA interaction by sodium chloride. The results indicated that the interaction of FtsZ with EzrA may have significant electrostatic contributions.

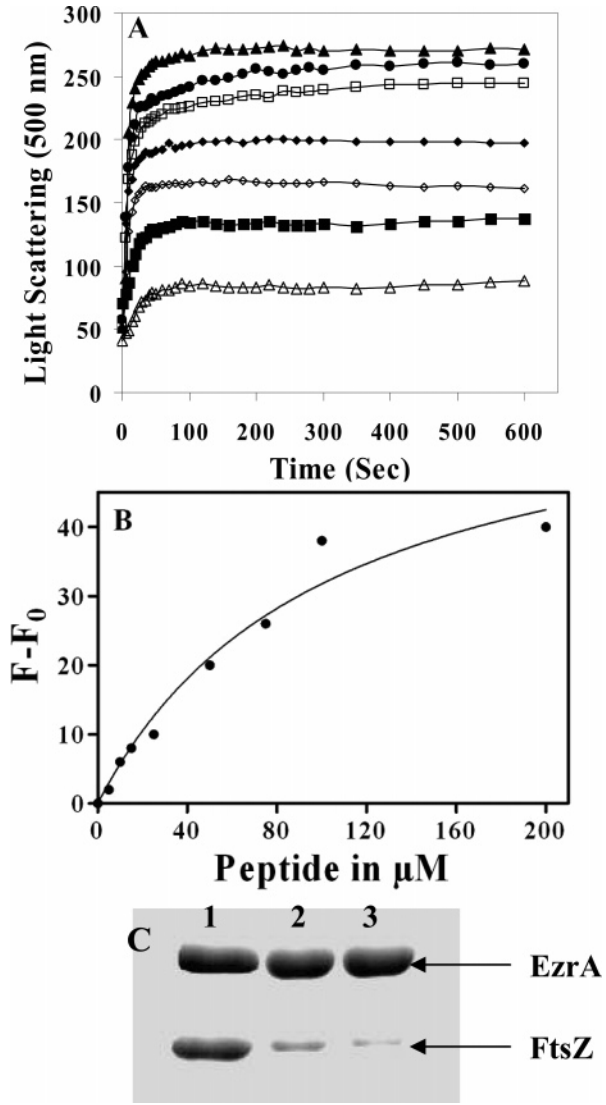

FIGURE 8: CTP17 suppressed the inhibitory effects of EzrA on the assembly of FtsZ. EzrA (7.2 μM) was incubated without or with different concentrations (10−100 μM) of CTP17 in 25 mM Pipes buffer, pH 6.8, for 30 min on ice. Then, FtsZ (14.4 μM) was added to the reaction mixtures and incubated for an additional 30 min on ice. The assembly reaction was started by adding 10 mM $MgCl_2$ and 1 mM GTP and transferring the mixtures to 37 °C for 10 min. Panel A shows the kinetics of FtsZ assembly in the absence (▲) or presence of 7.2 μM EzrA without (△) or with 10 μM (■), 25 μM (◇), 50 μM (◆), and 100 μM CTP17 (□), respectively. In the absence of EzrA, CTP17 (100 μM) had no effect on the assembly kinetics of FtsZ (●). Panel B shows the change in the fluorescence intensity of acrylodan−EzrA (1.2 μM) in the presence of different concentrations of CTP17. Panel C shows the Coomassie blue staining of the 10% SDS−PAGE of EzrA complexed with FtsZ in the absence of CTP17 (lane 1) or in the presence of 100 μM (lane 2) and 300 μM CTP17 (lane 3), respectively.

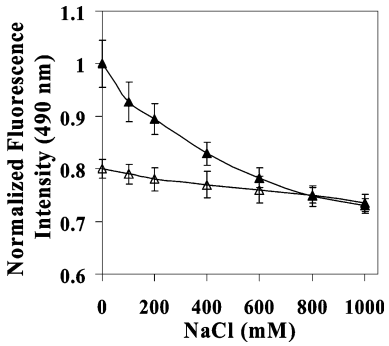

FIGURE 9: Effects of increasing ionic strength on the interaction between FtsZ and EzrA. The effect of increasing concentrations of NaCl on the fluorescence intensity of acrylodan−EzrA is shown in the absence (△) and presence (▲) of FtsZ.

DISCUSSION

The stability and positioning of the Z-ring at the midcell are crucial during cytokinesis in bacterial cell division. Both positive and negative regulators of FtsZ assembly influence the stability and positioning of the Z-ring. EzrA is known to prevent the formation of aberrant Z-rings in bacteria by modulating FtsZ assembly dynamics (*17*), and the negative regulation of the Z-ring by EzrA is thought to be required for the efficient cell division during the growth of *B. subtilis* (*18*, *34*). In this study, we found that EzrA increased the critical concentration of FtsZ assembly, reduced the assembly and bundling of the FtsZ protofilaments, and depolymerized the preformed FtsZ protofilaments. We also show direct interaction between FtsZ and EzrA proteins using size-exclusion chromatography, emphasizing that FtsZ forms a stable complex with EzrA. Further, we have provided evidence indicating that the binding site of EzrA on FtsZ resides at the extreme C-terminal tail (16 C-terminal residues) of FtsZ. The C-terminal interactions of FtsZ with EzrA were confirmed using a C-terminal peptide (365−382) of FtsZ. The peptide bound to EzrA, inhibited the binding of FtsZ to EzrA, and negated the inhibitory effects of EzrA on the assembly of FtsZ. The binding of EzrA with FtsZ decreased with the increasing ionic strength, suggesting that the binding of these proteins involves electrostatic interactions.

EzrA bound to soluble FtsZ at a single site with a dissociation constant of 4.3 ± 0.6 μM (Figure 7B). High concentrations of EzrA were required to inhibit FtsZ assembly, which precluded the possibility that EzrA inhibited FtsZ assembly by binding at or near the end of FtsZ protofilaments. EzrA was found to form a stable complex with soluble FtsZ monomers (Figure 5), and stoichiometric concentrations of EzrA were required to inhibit FtsZ assembly, suggesting that the inhibitory effects of EzrA on the assembly of FtsZ may be explained by the sequestration mechanism, wherein EzrA-bound FtsZ does not form polymers. EzrA was also found to increase the critical concentration of FtsZ assembly (Figure 3). The critical concentration of FtsZ assembly estimated using the concentration of unliganded FtsZ corroborates well with the idea that EzrA increases the critical concentration by forming a complex with FtsZ and depleting the pool of active FtsZ monomers. The concentration of EzrA in *B. subtilis* cells was estimated to be 10000−20000 molecules per cell (*17*). The high cellular concentration of EzrA also supports the idea that EzrA inhibits FtsZ assembly by sequestrating FtsZ monomers.

Earlier, EzrA has been shown to destabilize polymerized FtsZ in vivo in *B. subtilis* (*18*). It has also been suggested that EzrA contributes to the Z-ring remodeling by accelerating the disassembly of the Z-ring, such that in the absence of EzrA the slow disassembly of the Z-ring may reduce the concentration of free FtsZ monomers or protofilaments in the cytoplasm adversely affecting the efficiency of the Z-ring formation in the next round of cell division (*16*, *35*). The present study conforms to this suggestion as EzrA destabilized the FtsZ polymers and caused disassembly of the

preformed FtsZ bundles in vitro. In comparison, EzrA did not effectively disturb the FtsZ bundles formed in the presence of DEAE-dextran (*17*), which may be due to the fact that FtsZ forms highly stabilized polymers in the presence of DEAE-dextran (*36*).

The assembly dynamics of the Z-ring are determined primarily by GTP hydrolysis (*36*). SulA, which negatively regulates the Z-ring formation by inhibiting the GTPase activity, binds to the GTPase-activating T7 loop of FtsZ (*36*−39). Unlike SulA, EzrA has been observed to enhance the GTPase activity of FtsZ marginally despite lowering the GTP binding to FtsZ (*28*). The apparently contradictory effects of EzrA on FtsZ were accounted for by the suggestion that EzrA may alter the conformation of FtsZ. The GTP-binding interactions lie in the N-terminal domain of FtsZ, which is also involved in monomer−monomer interactions within a protofilament (*40*). The polymerization of the truncated FtsZ lacking 16 C-terminal residues was not inhibited by EzrA. Also, the bundles of truncated FtsZ were unaffected by EzrA as clearly seen under a transmission electron microscope. Further, the inhibitory effects of EzrA on FtsZ polymerization were countered by a 17-mer C-terminal peptide (365−382) of *B. subtilis* FtsZ, as the peptide directly interacted with EzrA. Therefore, the results unambiguously suggest that the primary binding site of EzrA is located in the 16-residue C-terminal tail of FtsZ. The conserved C-terminal tail of FtsZ has been shown to be required for interaction with other essential division proteins, FtsA and ZipA in *E. coli*, both of which are positive-acting factors (*21*).

FtsA, a conserved protein in prokaryotes, localizes at the midcell, and it has been suggested that FtsA induces the bundling of FtsZ protofilaments (*25*, *41*). It has been previously shown that FtsA interacts at the C-terminal tail of FtsZ (*25*). The binding site for the negative regulator EzrA and the positive regulator FtsA may thus partially overlap. The overlapping binding sites for EzrA and positive regulators may explain the formation of a medial Z-ring, as EzrA being uniformly distributed throughout the plasma membrane can prevent FtsZ assembly anywhere along the inner surface of the plasma membrane (*18*). The positive regulators like FtsA competing for the same site on FtsZ can overcome EzrA activity in a position-specific manner. This suggestion is consistent with the observation that the loss of EzrA results in cells with multiple Z-rings located at polar as well medial sites leading to the cell elongation and increase in percentage of filamentous cells of *B. subtilis* (*34*).

ACKNOWLEDGMENT

We thank SAIF, IIT Bombay, for providing the transmission electron microscopy facility. We sincerely thank Dr. P. A. Levin for the kind gift of the pRS3-*ezrA* construct and Dr. R. Mukhopadhyaya, Bhabha Atomic Research Centre, for helping in DNA sequencing.

REFERENCES

1. Michie, K. A., and Lowe, J. (2006) Dynamic filaments of the bacterial cytoskeleton, *Annu. Rev. Biochem. 75*, 467−492.
2. Errington, J., Daniel, R. A., and Scheffers, D. J. (2003) Cytokinesis in bacteria, *Microbiol. Mol. Biol. Rev. 67*, 52−65.
3. Rothfield, L., Justice, S., and Garcia-Lara, J. (1999) Bacterial cell division, *Annu. Rev. Genet. 33*, 423−448.
4. Lutkenhaus, J., and Addinall, S. G. (1997) Bacterial cell division and the Z ring, *Annu. Rev. Biochem. 66*, 93−116.
5. Nogales, E., Downing, K. H., Amos, L., and Lowe J. (1998) Tubulin and FtsZ form a distinct family of GTPases, *Nat. Struct. Biol. 6*, 451−458.
6. de Boer, P., Crossley, R., and Rothfield, L. (1992) The essential bacterial cell-division protein FtsZ is a GTPase, *Nature 359*, 254−256.
7. Scheffers, D. J., and Driessen, A. J. (2002) Immediate GTP hydrolysis upon FtsZ polymerization, *Mol. Microbiol. 43*, 1517−1521.
8. Yu, X. C., and Margolin, W. (1997) Ca^{2+}-mediated GTP-dependent dynamic assembly of bacterial cell division protein FtsZ into asters and polymer networks *in vitro*, *EMBO J. 16*, 5455−5463.
9. Mukherjee, A., and Lutkenhaus, J. (1998) Dynamic assembly of FtsZ regulated by GTP hydrolysis, *EMBO J. 17*, 462−469.
10. Mukherjee, A., and Lutkenhaus, J. (1994) Guanine nucleotide-dependent assembly of FtsZ into filaments, *J. Bacteriol. 176*, 2754−2758.
11. Hale, C. A., and de Boer, P. A. (1997) Direct binding of FtsZ to ZipA, an essential component of the septal ring structure that mediates cell division in *E. coli*, *Cell 88*, 175−185.
12. Mukherjee, A., and Lutkenhaus, J. (1999) Analysis of FtsZ assembly by light scattering and determination of the role of divalent metal cations, *J. Bacteriol. 181*, 823−832.
13. Mukherjee, A., Santra, M. K., Beuria, T. K., and Panda, D. (2005) A natural osmolyte trimethylamine *N*-oxide promotes assembly and bundling of the bacterial cell division protein, FtsZ and counteracts the denaturing effects of urea, *FEBS J. 272*, 2760−2772.
14. Santra, M. K., Beuria, T. K., Banerjee, A., and Panda, D. (2004) Ruthenium red-induced bundling of bacterial cell division protein, FtsZ, *J. Biol. Chem. 279*, 25959−25965.
15. Gonzalez, J. M., Jiménez, M., Velez, M., Mingorance, J., Andreu, J. M., Vicente, M., and Rivas. G. (2003) Essential cell division protein FtsZ assembles into one monomer-thick ribbons under conditions resembling the crowded intracellular environment, *J. Biol. Chem. 278*, 37664−37671.
16. Anderson, D. E., Gueiros-Filho, F. J., and Erickson, H. P. (2004) Assembly dynamics of FtsZ rings in *Bacillus subtilis and Escherichia coli* and effects of FtsZ-regulating proteins, *J. Bacteriol. 186*, 5775−5781.
17. Haeusser, D. P., Schwartz, R. L., Smith, A. M., Oates, M. E., and Levin, P. A. (2004) EzrA prevents aberrant cell division by modulating assembly of the cytoskeletal protein FtsZ, *Mol. Microbiol. 52*, 801−814.
18. Levin, P. A., Kurtser, I. G., and Grossman, A. D. (1999) Identification and characterization of a negative regulator of FtsZ ring formation in *Bacillus subtilis*, *Proc. Natl. Acad. Sci. U.S.A 96*, 9642−9647.
19. Gueiros-Filho, F. J., and Losick, R. (2002) A widely conserved bacterial cell division protein that promotes assembly of the tubulin-like protein FtsZ, *Genes Dev. 16*, 2544−2556.
20. Descoteaux, A., and Drapeau, G. R. (1987) Regulation of cell division in *Escherichia coli* K-12: probable interactions among proteins FtsQ, FtsA, and FtsZ, *J. Bacteriol. 169*, 1938−1942.
21. Hale, C. A., Rhee, A. C., and de Boer, P. A. (2000) ZipA-induced bundling of FtsZ polymers mediated by an interaction between C-terminal domains, *J. Bacteriol. 182*, 5153−5166.
22. Bi, E. F., and Lutkenhaus, J. (1991) FtsZ ring structure associated with division in *Escherichia coli*, *Nature 354*, 161−164.
23. Bi, E. F., and Lutkenhaus, J. (1993) Cell division inhibitors SulA and MinCD prevent formation of the FtsZ ring, *J. Bacteriol. 175*, 1118−1125.
24. Low, H. H., Moncrieffe, M. C., and Lowe, J. (2004) The crystal structure of ZapA and its modulation of FtsZ polymerization, *J. Mol. Biol. 341*, 1839−1852.
25. van den Ent, F., and Lowe, J. (2000) Crystal structure of the cell division protein FtsA from *Thermotoga maritima*, *EMBO J. 19*, 5300−5307.
26. Rothfield, L., Taghbalout, A., and Shih, Y. L. (2005) Spatial control of bacterial division-site placement, *Nat. Rev. Microbiol. 12*, 959−968.
27. Levin, P. A., Schwartz, R. L., and Grossman, A. D. (2001) Polymer stability plays an important role in the positional regulation of FtsZ, *J. Bacteriol. 183*, 5449−5452.
28. Chung, K. M., Hsu, H. H., Yeh, H. Y., and Chang, B. Y. (2006) Mechanism of regulation of prokaryotic tubulin-like GTPase FtsZ by membrane protein EzrA, *J. Biol. Chem. 282*, 14891−14897.

29. Bradford, M. M. (1976) A rapid and sensitive method for the quantitation of microgram quantities of protein utilizing the principle of protein-dye binding, *Anal. Biochem. 72*, 248−254.
30. Lu, C, Stricker, J., and Erickson, H. P. (1998) FtsZ from *Escherichia coli*, *Azotobacter vinelandii*, and *Thermotoga maritima*−quantitation, GTP hydrolysis, and assembly, *Cell Motil. Cytoskeleton 40*, 71−86.
31. Beuria, T. K., Krishnakumar, S. S., Sahar, S., Singh, N., Gupta, K., Meshram, M., and Panda, D. (2003) Glutamate-induced assembly of bacterial cell division protein FtsZ, *J. Biol. Chem. 278*, 3735−3741.
32. Huang, C. Y. (1982) Determination of binding stoichiometry by the continuous variation method: the Job plot, *Methods Enzymol. 87*, 509−525.
33. Ward, L. D. (1985) Measurement of ligand binding to proteins by fluorescence spectroscopy, *Methods Enzymol. 117*, 400−414.
34. Chung, K. M., Hsu, H. H., Govindan, S., and Chang, B. Y. (2004) Transcription regulation of *ezrA* and its effect on cell division of Bacillus subtilis, *J. Bacteriol. 186*, 5926−5932.
35. Stricker, J., Maddox, P., Salmon, E. D., and Erickson, H. P. (2002) Rapid assembly dynamics of the *Escherichia coli* FtsZ-ring demonstrated by fluorescence recovery after photobleaching, *Proc. Natl. Acad. Sci. U.S.A. 99*, 3171−3175.
36. Trusca, D., Scott, S., Thompson, C., and Bramhill, D. (1998) Bacterial SOS checkpoint protein SulA inhibits polymerization of purified FtsZ cell division protein, *J. Bacteriol. 180*, 3946−3953.
37. Mukherjee, A., Cao, C., and Lutkenhaus, J. (1998) Inhibition of FtsZ polymerization by SulA, an inhibitor of septation in *E. coli*, *Proc. Natl. Acad. Sci. U.S.A. 95*, 2885−2890.
38. Cordell, S. C., Robinson, E. J., and Lowe, J. (2003) Crystal structure of the SOS cell division inhibitor SulA and in complex with FtsZ, *Proc. Natl. Acad. Sci. U.S.A. 100*, 7889−7894.
39. Lowe. J., and Amos, L. A. (1998) Crystal structure of the bacterial cell-division protein FtsZ, *Nature 391*, 203−206.
40. Pichoff, S., and Lutkenhaus, J. (2001) Escherichia coli division inhibitor MinCD blocks septation by preventing Z-ring formation, *J. Bacteriol. 183*, 6630−6635.
41. Ma, X., and Margolin, W. (1999) Genetic and functional analyses of the conserved C-terminal core domain of *Escherichia coli* FtsZ, *J. Bacteriol. 181*, 7531−7544.

BI700710J